Solution Structure of Monomeric Peptide YY Supports the Functional Significance of the PP-Fold[†,‡]

David A. Keire,[*,§,||] Mitsuo Kobayashi,[||] Travis E. Solomon,[§] and Joseph R. Reeve, Jr.[§]

CURE Digestive Diseases Research Center, Greater Los Angeles Veterans Healthcare System, Los Angeles, California 90073, Digestive Diseases Division, UCLA School of Medicine, Los Angeles, California 90023, and Division of Immunology, The Beckman Research Institute of the City of Hope, 1450 East Duarte Road, Duarte, California 91010-0269

Received November 8, 1999; Revised Manuscript Received May 22, 2000

ABSTRACT: Peptide YY (PYY) belongs to a family of peptides including neuropeptide Y (NPY) and pancreatic peptide (PP) that regulate numerous functions through both central and peripheral receptors. The solution structure of these peptides is hypothesized to be critically important in receptor selectivity and activation, based on prior demonstration of a stable tertiary conformation of PP called the "PP-fold". Circular dichroism (CD) spectra show a pH-dependent structural transition in the pH range 3−4. Thus we describe the tertiary structure of porcine PYY in water at pH 5.5, 25 °C, and 150 mM NaCl, as determined from 2D ^{1}H NMR data recorded at 500 MHz. A constraint set consisting of 396 interproton distances from NOE data was used as input for distance geometry, simulated annealing, and restrained energy minimization calculations in X-PLOR. The RMSDs of the 20 X-PLOR-generated structures were 0.71 ± 0.14 and 1.16 ± 0.17 Å, respectively, for backbone and heavy atom overlays of residues 1−34. The resulting structure consists of two C-terminal helical segments from residues 17 to 22 and 25 to 33 separated by a kink at residues 23, 24, and 25, a turn centered around residues 12−14, and the N-terminus folded near residues 30 and 31. The well-defined portions of the PYY structure reported here bear a marked similarity to the structure of PP. Our findings strongly support the importance of the stable folded structure of this family of peptides for binding and activation of Y receptor subtypes.

Peptide YY (PYY),[1] neuropeptide Y (NPY), and pancreatic polypeptide (PP) constitute a family of C-terminally amidated peptides involved in the regulation of gastrointestinal function, blood pressure, and feeding behavior (*1*). The ability of these peptides to selectively bind and activate Y receptor subtypes has been postulated to depend strongly on a stable solution structure, the so-called "PP-fold" (*2*). Support for this hypothesis was found when the solution structure of bovine PP was reported to be similar to the crystal structure of aPP (*3*). The primary sequences of PYY and NPY share 19/36 and 20/36 residues with aPP (Figure 1), and this approximate 50% sequence homology has been taken as evidence that all of these peptides share a similar stable solution structure.

```
          5    10   15   20   25   30   35
PYY-  YPAKP EAPGE DASPE ELSRY YASLR HYLNL VTRQR Y#
NPY-  YPSKP DNPGE DAPAE DLARY YSALR HYINL ITRQR Y#
aPP-  GPSQP TYPGD DAPYE DLIRF YDDLQ QYLNV VTRHR Y#
```

FIGURE 1: Primary sequences of porcine PYY, porcine NPY, and avian PP with the amino acid changes from PYY in NPY and aPP in boldface and underlined. The # symbol denotes the C-terminal amide group.

These peptides express their bioactivity via a family of G-protein-coupled Y receptors (*1*, *4*). On the basis of functional and ligand binding studies, it is now widely accepted that PYY, NPY, and PP bind to and activate at least six Y receptor subtypes (*5*−*7*). Four of these Y receptor subtypes, Y_1, Y_2, Y_4, and Y_5, have been recently cloned (*8*−*13*). Two other putative subtypes, including NPY- (Y_3-) and PYY-preferring receptor subtypes, have been characterized pharmacologically (*6*, *14*, *15*).

Of these subtypes, NPY and PYY bind to Y_1, Y_2, and Y_5 receptors with high (sub-nanomolar) affinities, while PP binds poorly (*1*). [Pro^{34}]PYY (or [Pro^{34}]NPY) bind to Y_1 receptors with high affinity but bind poorly to Y_2 receptors (*16*, *17*). Conversely, PYY(3−36) [or NPY(3−36)], endogenous molecular forms of PYY (or NPY) (*18*, *19*), bind with high affinity to Y_2 receptors but poorly at Y_1 receptors (*16*).

Our previous work has shown that the differences in the Y_1 and Y_2 receptor binding affinities of PYY, [Pro^{34}]PYY, and PYY(3−36) are correlated with secondary and tertiary structure changes (*17*). We proposed that these tertiary structure changes (in addition to the primary structure

[†] This research was supported by CURE Digestive Diseases Research Center Grant DK41301 and utilized the Peptide Biochemistry and Molecular Probes Core. This research was also supported by the Medical Research Service of the Veterans Health Service and by NIH Grant DK-33850.

[‡] The structure coordinates have been deposited in the Brookhaven Protein Data Bank (filename 1QBF).

* Address correspondence to this author at the UCLA/CURE Digestive Diseases Research Center, Building 115, Room 115, Greater Los Angeles Veterans Health Care System, 11301 Wilshire Blvd., Los Angeles, CA 90073. Phone: (310)-268-3935. Fax: (310)-268−4963. E-mail: dkeire@ucla.edu.

[§] Greater Los Angeles Veterans Healthcare System and UCLA School of Medicine.

[||] The Beckman Research Institute of the City of Hope.

[1] Abbreviations: PYY, peptide YY; NPY, neuropeptide Y; PP, pancreatic peptide; NMR, nuclear magnetic resonance; CD, circular dichroism; NOE, nuclear Overhauser effect; NOESY, nuclear Overhauser effect spectroscopy; TOCSY, total correlation spectroscopy; DQF-COSY, double-quantum-filtered correlation spectroscopy; RMSD, root-mean-square deviation.

10.1021/bi992576a CCC: $19.00
Published on Web 07/21/2000

Table 1: Selected Structural Studies on PP Family Peptides in Aqueous Solution

peptide[a]	monomer−dimer K_d (M)[b]	solution conditions	methods	results	ref
aPP		crystal	X-ray	3D structure (dimer)	*34*
bPP		pH 4.6, 28 °C, 7 mM peptide	NMR	3D solution structure (monomer)	*3*
pNPY	2×10^{-6}	pH 7.4, ~22 °C, 0.16 M KCl	CD	forms dimers	*39*
pNPY		pH 3.1, 37 °C, 4 mM peptide, 50 mM acetate	NMR and CD	dimer (pH-dependent structure)	*31*
pNPY	1.6×10^{-6}	pH 2−8, 20 °C, 50 mM acetate or Tris	fluorescence (Tyr)	dimer	*40*
		pH 3.2, 37 °C, 4 mM peptide, 50 mM acetate	NMR	3D solution structure (dimer)	
pNPY	1.9×10^{-6}	pH 7.5, 25 °C, 150 mM NaCl	CD	dimer	*41*
hNPY		pH 3.2, 37 °C, 4 mM peptide	NMR	3D solution structure (aPP-like monomer)	*21*
hNPY	1.4×10^{-4}	pH 3.1, 18 °C, 0.1 M NaCl	AU[c]	NPY is 66% dimer at 4 mM	*22*
		pH 3.2, 37 °C, 4 mM peptide	NMR	3D solution structure (dimer)	
hNPY	$\sim 2 \times 10^{-6}$	pH 7.2, 25 °C, 10 mM Tris	CD and NMR	pH- and temperature-dependent structure	*42*
pPYY	2.1×10^{-2}	pH 5, 21 °C, 0.15 M KCl	AU	PYY is 92% monomer at 1 mM	*17*
pPYY		pH 5.5, 25 °C, 1.0 mM peptide, 0.15 M NaCl	NMR	3D solution structure (aPP-like monomer)	this work
		0.3 mM peptide	CD	pH-dependent structure	this work

[a] Key: a = avian, b = bovine, p = porcine, and h = human. [b] Monomer−dimer dissociation constant (K_d = [M][M]/[MM]). [c] Analytical ultracentrifugation sedimentation equilibrium analysis.

differences of the three peptides) influence the receptor subtype selectivity of PYY. Similarly, Beck-Sickinger et al. proposed that NPY interacts with the Y_1 and Y_2 receptor via different conformations and different residues (*20*).

To better examine the role of structure in PYY bioactivity, we have solved the 3D aqueous solution structure of PYY. PYY has several advantages over PP and NPY for structure−function studies at Y_1 and Y_2 receptors. PP binds poorly to Y_1 and Y_2 receptors. Numerous structural studies have been performed on PP and NPY; those studies performed on peptides in aqueous solution are summarized in Table 1. These studies show that NPY has a propensity to form dimers at the millimolar concentrations necessary for structure determination. In addition, two studies disagree as to the monomer−dimer nature of NPY at millimolar concentrations, reporting different 3D structures under identical solution conditions (*21*, *22*). We have previously reported that PYY is mainly monomeric in 1 mM aqueous solution at pH 5 (*17*), whereas under similar conditions NPY is dimeric (Table 1). Under physiological conditions (i.e., nanomolar peptide, pH 7.4, and 0.15 M NaCl), NPY and PYY will express their activity as monomers. Thus the 3D structure determined in this work most likely represents the monomeric solution form of PYY that binds to Y receptors. The current work tested and confirmed the hypothesis that PYY exists in a stable, folded structure similar to that of PP.

MATERIALS AND METHODS

Experimental Procedure. Porcine PYY was purchased from Peninsula Laboratories (Belmont, CA) and used as delivered. On the basis of the data supplied by Peninsula, the peptide was >95% pure as evaluated by analytical reverse-phase HPLC. The pH of the H_2O solutions was adjusted between 5 and 6 by the addition of HCl and NaOH; measurements were performed using an Orion Model 601 pH meter fitted with a combination electrode for 5 mm NMR tubes (Ingold Electrodes, Wilmington, MA). Standard aqueous buffers were used for electrode calibration at pH 4 and 7.

CD Spectropolarimetry. The circular dichroism experiments were performed on a Jasco J-600 spectropolarimeter (Easton, MD). A 0.1 mm cell was used with micromolar concentrations of peptide. The ellipticity for each sample was measured over a wavelength range of 180−300 nm, with 10 scans averaged and a sweep rate of 20 nm/min.

NMR Studies. NMR experiments were performed on a Varian Unity Plus 500 MHz instrument(Varian Instruments, Palo Alto, CA) with probe air temperature regulated at 25 °C. Solutions for NMR analysis of PYY were made at approximately 1 mM peptide concentration in 750 μL of 90% H_2O/10% D_2O. Chemical shift assignments for PYY in solution were obtained by the standard method (*23*) using total correlation spectroscopy [TOCSY (*24*)], nuclear Overhauser effect spectroscopy [NOESY (*25*)], and double-quantum-filtered correlation spectroscopy [DQF-COSY (*26*)] pulse sequences. All chemical shifts were reference to external 2,2-dimethyl-2-silapentane-5-sulfonic acid in D_2O.

Phase-sensitive NOESY data were used for conformational analysis of the PYY solutions, with 4K points collected in t_2 (32 transients per increment), 100 or 200 ms mixing times, and 512 complex points in t_1 (*27*). The transmitter channel was used for excitation and observation of the 6000 Hz proton frequency range as well as presaturation of the H_2O signal. Data were processed with zero filling to 8K points in F_2, 2K points in F_1, and 90° shifted sine bell apodization functions in both F_1 and F_2.

Structure Calculations. Structures for PYY were determined using X-PLOR software, Version 3.1 (*28*). For PYY, 100 and 200 ms NOESY experiments provided the 396 distance restraints needed for X-PLOR 3D structure calculations. Strong, medium, and weak distance restraints were input as 1.8−4.0, 1.8−5.0, and 1.8−6.0 Å distance ranges, respectively, and standard pseudoatom corrections were used where appropriate (*29*). The constraint set for PYY contained 135 (i, i+1), 20 (i, i+2), 29 (i, i+3), 19 (i, i+4), and 37 ($\geq i$, i+5) NOEs between protons on various residues. The greater than or equal to i, i+5 NOEs can only be present in a stable folded conformation of PYY.

In addition, nine hydrogen bond constraints were included on the basis of the presence of three or more sequential i, i+3, or i, i+4 NOEs (Figure 5). Because of the pH and temperature dependence of the PYY chemical shifts, additional

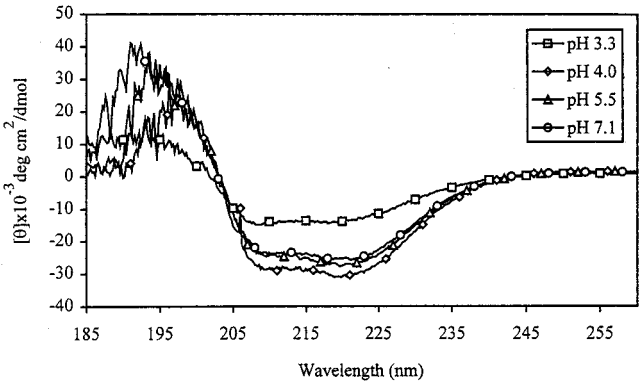

FIGURE 2: Plot of the CD molecular ellipticity from 185 to 260 nm of 0.3 mM PYY at pH 3.3 (squares), 4.0 (diamonds), 5.5 (triangles), and 7.1 (circles) in H_2O.

evidence for the presence of hydrogen-bonded residues by amide exchange rate measurements was not available (see Results and Discussion). The hydrogen bond constraints were included for residues 17−21 and 26−30. For each hydrogen bond determined from the NOE connectivities, two distances were input into the structure calculations: 1.8−2.5 Å from the backbone carbonyl oxygen atom of the N-terminal residue to the amide hydrogen of the *i* to *i*+4 residue and 1.8−3.5 Å from the carbonyl on the N-terminal residue to the amide nitrogen of the *i* to *i*+4 residue.

These constraints were used for the calculation of PYY structures satisfying the distance boundaries. One hundred embedded distance geometry structures were obtained using the "dgse" protocol. The simulated annealing protocol "dgsa" was employed to regularize the structures, with a force constant of 50 kcal on the NOE-derived distance restraints and the nine hydrogen-bonding constraints (*28*, *30*). The parameter file "parallhdg.pro" was employed in this procedure. Once structures were regularized in this fashion, they were subjected to an additional 10 ps of simulated annealing by the "refine" protocol. The energy of each regularized and refined structure was then minimized for 200 cycles. Out of the resulting 200 structures, 20 were chosen that had the lowest NOE energies (Figure 7). X-PLOR-generated structures were visualized with the program Insight (Version 98; Biosym Technologies, San Diego, CA).

RESULTS

pH Dependence of PYY Structure. CD spectra indicate that the solution structure of PYY is pH dependent. For CD studies, spectra were collected at room temperature for various pHs (3.3, 4.0, 5.5, 6.0, 7.1, and 8.4) of 0.3 mM PYY in aqueous solution; selected spectra are shown in Figure 2. The greatest helical character and the lowest observed ellipticity at 222 nm occurs at pH 4 and decreases at lower and higher pHs. All of the PYY spectra showed helical character with a positive band at [+]195 nm and negative bands at [−]208, and [−]222 nm. The intensity of these bands is pH dependent. For example, the molecular ellipticity of PYY at 222 nm at pH 3.3 (-13.3×10^3 deg cm^2 dmol^{-1}) was ca. 56−40% lower than the values observed from pH 4 to pH 8.4 (-30.1×10^3 to -22.4×10^3 deg cm^2 dmol^{-1}).

NMR Data. The NMR chemical shift assignments and NOE data were collected at a pH of 5.5 to as closely as possible mimic the physiological charge state of PYY without losing significant amide proton signal intensity due to amide exchange. The 2D NOESY or TOCSY spectra showed no evidence of multiple conformations of the peptide. The presence of $C_\alpha H(i-1)$ to Pro# $C_\delta H$ NOE connectivities and the absence of $C_\alpha H(i-1)$ to Pro# $C_\alpha H$ NOE connectivities indicate that proline residues P2, P5, and P8 are in the trans conformation. No data were available for residue P14 because proton signals for the P14 $C_\delta H$ protons were not found in either the NOESY or TOCSY spectra.

The 1D NMR spectra amide and aromatic proton signals of PYY were sensitive to temperature, pH, and concentration. For example, 500 MHz 1D NMR spectra collected at pH 3.4 and 5.7 showed significant differences in the pattern of aromatic and amide proton signals (data not shown). The changes observed in these signals can be attributed to changes in the monomer−dimer equilibrium constant and/or structure changes in the monomer (i.e., increasing or decreasing helix stability).

The standard NMR methods that supply evidence for hydrogen bonding and the presence of secondary structure could not be used because of the pH and temperature dependence of the PYY chemical shifts. At the pH and temperature that the NMR structure data were collected (pH 5.5 and 25 °C), the amide proton exchange rates were too rapid to measure by 1D methods. In addition, at lower temperatures or pHs where the amide exchange rates are decreased, the chemical shift assignments were sufficiently altered such that unambiguous identification of slowly exchanging amides was not possible. Furthermore, measurement of NH to $C_\alpha H$ scalar coupling in either 1D or 2D data was not possible due to overlap of amide resonances and broad line widths.

NMR Chemical Shift Assignments. ^{1}H chemical shift assignments for PYY in pH 5.5 aqueous solution were determined at 500 MHz and 25 °C by NMR methods (Supporting Information, Table 2). Chemical shifts for the $C_\alpha H$ proton signals of PYY in solution are plotted versus the random-coil solution-state chemical shifts of Wuthrich (*23*) in Figure 3. A series of chemical shifts that differ by more than ±0.2 ppm for the $C_\alpha H$ protons indicate a stable folded structure. These chemical shift differences indicate a nonrandom coil solution conformation for PYY, which is consistent with the CD data.

2D NOESY Spectra. The chemical shift assignments found in this work were used in conjunction with 2D NOESY data to obtain distance information for protons in PYY. Peaks at the intersection of two proton chemical shift assignments (cross-peaks) indicate protons that are within 5 Å of each other. A region of a NOESY spectrum of PYY showing the sequential NH−NH backbone connectivities is presented in Figure 4, with the various cross-peaks labeled by residue number. A stable folded structure is indicated by the presence of NH−NH cross-peaks between residues throughout the peptide. Some sequential connectivities are not visible due to (1) the presence of proline residues or (2) amide chemical shift differences that are too small.

The observed sequential NH−NH connectivities and the location of the *i*, *i*+2, *i*, *i*+3, *i*, *i*+4, and *i*, *i*+5 connectivities from the 100 and 200 ms NOESY spectra of PYY are summarized in Figure 5. Most of the medium-range connectivities are from side-chain proton to side-chain proton interactions because of the extensive overlap in the NH to

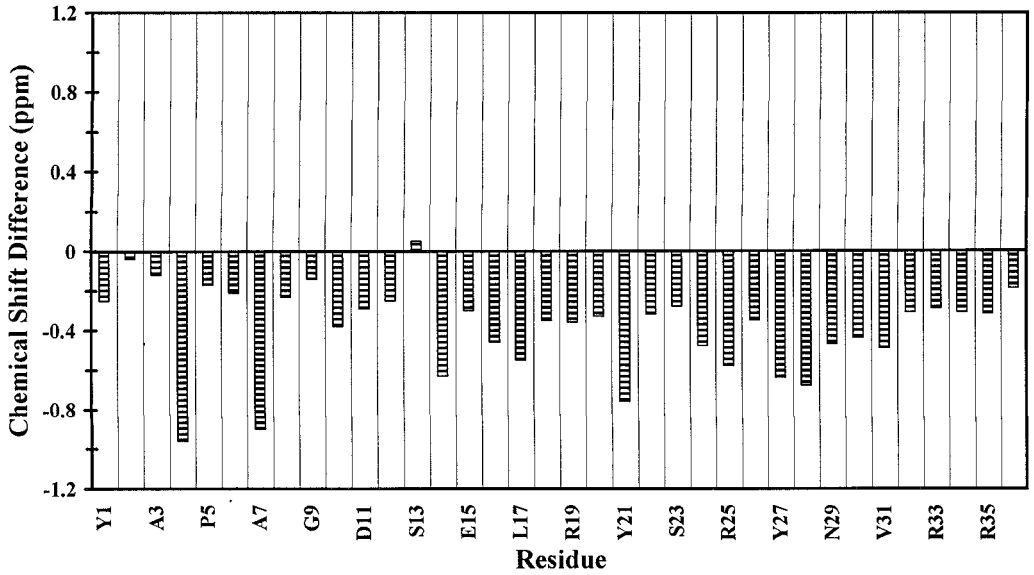

FIGURE 3: Plot of the differences in the chemical shift values of the $C_\alpha H$ protons of PYY in 90% H_2O/10% D_2O and pH 5.5 minus the random coil chemical shifts (*23*).

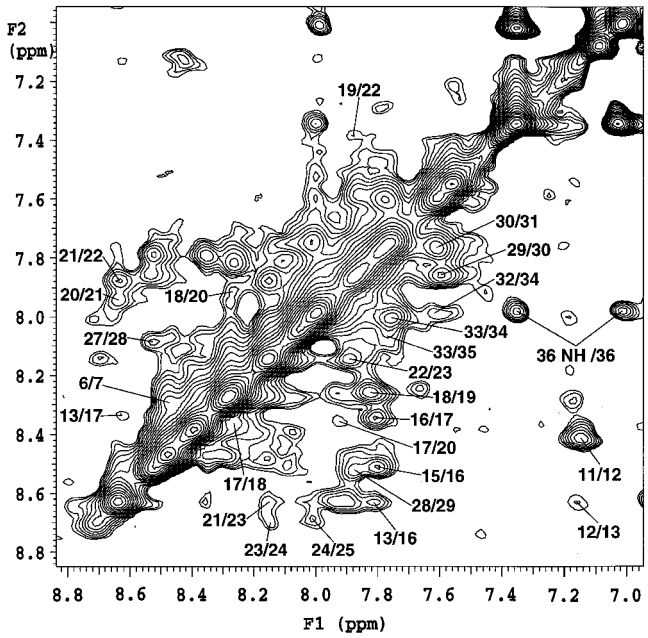

FIGURE 4: NH to NH proton (7.0−8.8 ppm) correlation region of a 200 ms 2D NOESY spectrum acquired on a solution of 1 mM PYY at pH 5.5 and 25 °C with 150 mM NaCl in 90% H_2O/10% D_2O. Selected cross-peaks are labeled to indicate through-space magnetization transfer between amide protons on different residues.

$C_\alpha H$ fingerprint region of the NOESY spectra. The NOE data in Figure 5 suggest helical character from residues L17 to L24 with a break followed by another helical segment from H26 to T32 (series of three or more *i*, *i*+3 and *i*, *i*+4 NOE connectivities are indicative of a helical structure). These results are in general agreement with the chemical shift analysis of the C-terminal portion of PYY.

Also observed in the 100 and 200 ms NOESY spectra are 37 NOE connectivities between protons on residues separated by five or more amino acids in the primary sequence. A selected region of the 100 ms NOESY spectrum is presented in Figure 6; it contains a number of cross-peaks between aromatic side chains and the β, γ, and δ protons of other residues. Cross-peak examples include the ϵ proton of Y20 (NOEs to P5 β and γ, P8 γ and δ, and A7 β protons), the ϵ and δ protons of Y27 (NOEs to V31 γ and T32 γ protons), and Y1 δ (NOE to the L30 δ protons). These and the other long-range NOEs clearly define the juxtaposition of the N- and C-terminal regions of PYY.

Tertiary Structure Determination. X-PLOR structure calculations were based on a set of 396 NOEs. This set consisted of 203 NOEs between protons of residues separated by four or fewer residues in the primary sequence of PYY, 37 NOEs between protons on residues five or more positions apart, and 155 intraresidue NOEs. These NOEs were derived from 100 and 200 ms NOESY spectra and classified into strong (1.8−4.0 Å), medium (1.8−5.0 Å), and weak (1.8−6.0 Å) distance categories on the basis of comparison of their cross-peak volumes with Tyr $C_\delta H$ to $C_\epsilon H$ cross-peak volumes. The upper limits of distances involving NOEs between more than one proton were modified with pseudoatoms where appropriate (*29*).

In addition to the NOE distance restraints, nine backbone CO−HN hydrogen bond distance restraints were included in the input distance list to the X-PLOR program. These distance restraints were based on the presence of three or more sequential *i*, *i*+3 and/or *i*, *i*+4 NOEs (Figure 5). The nine hydrogen bond distance restraints were from the carbonyl oxygen of residues 17−21 and 26−30 to the amide proton of the amino acid four residues toward the C-terminus. For these bonds a 1.8−2.5 Å distance restraint was used between the N-terminal residue carbonyl oxygen and the *i* to *i*+4 residue amide proton and a 1.8−3.5 Å distance restraint from the carbonyl oxygen to the amide nitrogen.

The constraint set above provided the input list to the X-PLOR program. Two hundred initial structures were generated by the distance geometry protocol, regularized by simulated annealing, and further refined by molecular dynamics (see Materials and Methods). An overlay was produced of the 20 best structures that had the lowest NOE energies. Figure 7 depicts a stereoview of the backbone (NH, $C_\alpha H$, CO) overlay and a stereoview of the mean conformation of these 20 structures. The 20 calculated structures have RMSDs of 0.71 ± 0.14 and 1.16 ± 0.17 Å for backbone and heavy atom overlays, respectively, of residues 1−34. A plot show-

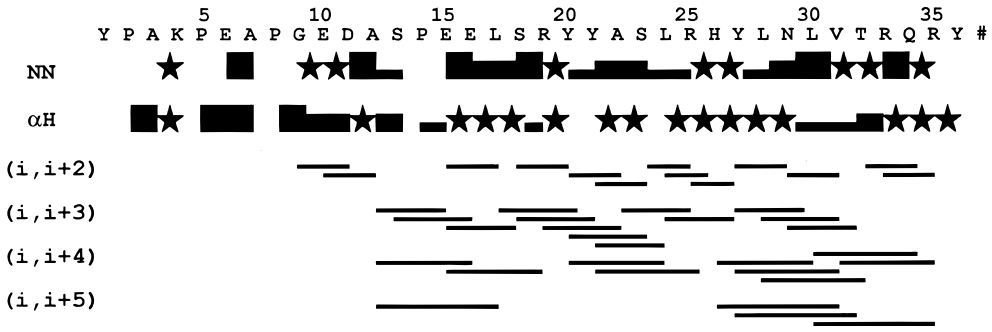

FIGURE 5: Selected NOE data used in the calculation of the tertiary structure of PYY in H_2O at pH 5.5, 25 °C, and 150 mM NaCl. A bar indicates the NOE connectivity between protons on different residues. The filled bars indicate the categorization of the NOE as a strong, medium, or weak distance restraint. Stars identify connectivities that were not observed because of chemical shift degeneracy. NOEs for protons between *i*, *i*+2, *i*, *i*+3, *i*, *i*+4, and *i*, *i*+5 are also shown but without categorization into strong, medium, and weak distances.

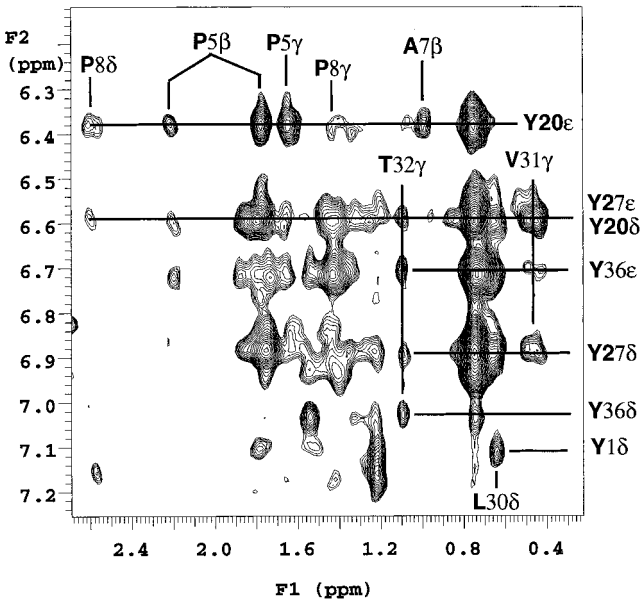

FIGURE 6: Aromatic (6.2−7.2 ppm) to β, γ, and δ (0.4−2.6 ppm) proton correlation region of a 100 ms 2D NOESY spectrum acquired on a solution of 1 mM PYY at pH 5.5 and 25 °C with 150 mM NaCl in 90% H_2O/10% D_2O. Selected cross-peaks are labeled to indicate through-space magnetization transfer between protons on different residues.

ing the average side-chain and backbone RMS deviation of the individual residues of PYY from the mean structure is shown in Figure 8. The mean energies of the 20 lowest NOE energy structures from the X-PLOR calculations (in kilocalories) are as follows: total energy 81 ± 5, bonds 5.1 ± 0.5, angles 40.9 ± 2.4, impropers 7.3 ± 0.8, van der Waals 11 ± 2, and NOEs 17 ± 2.

In the process of calculating the final set of structures (Figure 7), it became evident that multiple conformers existed for the turn region of PYY (residues 9−25). A set of NOE-based distance restraints was consistently violated in this portion of the peptide when distance upper bounds of 2.5, 3.5, and 5 Å were used for strong, medium, and weak NOEs. To obtain the lowest energy set of structures (described above), the upper distance boundaries were increased (to 4, 5, and 6 Å) and those NOEs that violated the larger upper distance boundaries were removed (27 of the observed NOEs were removed in this process) to obtain the final set of distance constraints.

DISCUSSION

We used CD and NMR methods to examine the solution structure of synthetic PYY. The goal of our studies was to determine whether the marked differences in the primary sequence of PYY from aPP and NPY still allowed a stable PP-fold in aqueous solution. Our results indicate that there is a remarkable degree of identity in tertiary structure between PYY and PP.

Initial structural studies were done using CD; the data indicate that marked changes in PYY helical content occur in the pH range of 3.3−4.0 with less dramatic changes between pH values of 4.0 and 8.4. Residues in PYY that are titrated in this pH range include E6, E10, D11, E15, E16, and H26. The titration of the side-chain carboxylic acid groups of the aspartate and glutamate (pK_a ca. 4.0) residues likely accounts for the major changes in helicity between pH 3 and pH 4. By contrast, the deprotonation of the side-chain ring nitrogen of the histidine at position 26 (pK_a ca. 6.5) probably makes a minimal contribution to this shift because of its higher pK_a. Deprotonation of the acidic residues may influence the stability of the C-terminal helix directly or by structural changes caused by dimer formation at low pH. Of note, Saudek and Pelton have also reported an observation of pH-dependent CD spectra for NPY at two pH values (3.1 vs 7.4), although no differences were observed in the 1D NMR spectra (*31*). Our experimental data on PYY narrow the pH range of the helicity shift to deprotonation of the acidic residues. The pH-dependent helicity change in NPY observed by Saudek and Pelton probably results from the same deprotonation step as PYY, because NPY and PYY have identical distributions of acidic residues.

The chemical shifts we observed indicate the presence of a helix in the C-terminal half of the peptide and nonrandom coil character in the N-terminal half of the peptide. The C-terminal helix is suggested by the consecutive $C_\alpha H$ downfield shifts of greater than 0.2 ppm from random coil chemical shifts from P14 to R35 (*23*, *32*). In addition, a nonhelical and nonrandom coil conformation for the N-terminal region of the peptide is consistent with the greater than 0.8 ppm downfield shifts from their random coil values of the N-terminal residues K4 and A7 $C_\alpha H$ protons.

The accuracy of the calculated structure is supported by the ring current shifts observed for side-chain protons in the vicinity of the Y1, Y20, H26, and Y27 residues. Ring current shifts arise from the diamagnetic anisotropy of the aromatic rings and often are the major contributing factor to the

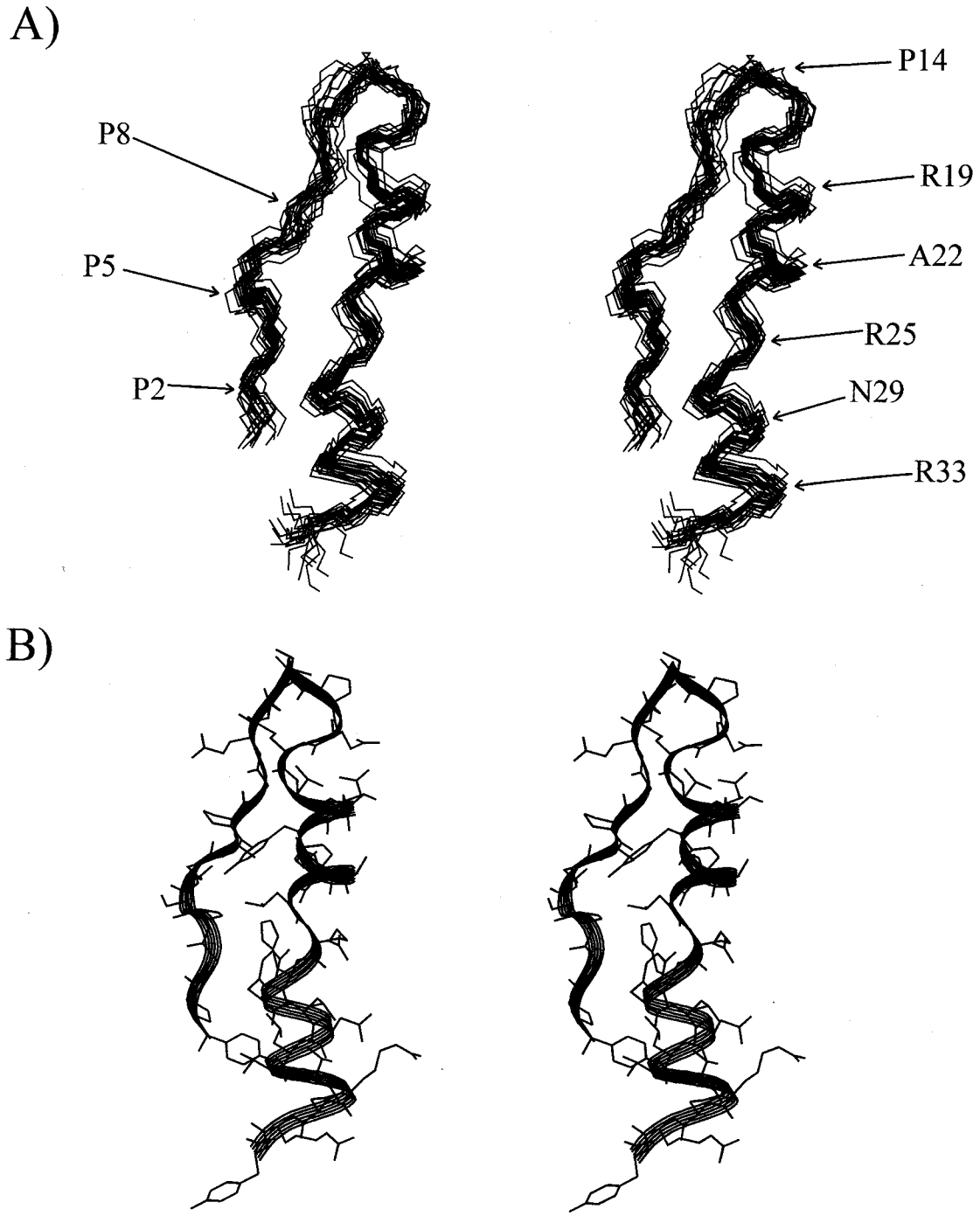

FIGURE 7: Stereoviews of (A) the superposition of 20 coordinate sets of the backbone atoms of residues 1−34 and (B) a heavy atom representation of the mean coordinate set derived from the 20 structures calculated with X-PLOR from 2D NOESY data on 1 mM PYY at pH 5.5 and 25 °C with 150 mM NaCl in 90% H_2O/10% D_2O. Selected residues are labeled, and the mean structure has a ribbon overlay of the backbone conformation.

observed conformation-dependent chemical shifts of side-chain protons (*33*). This is particularly noticeable for the P8 γ and δ protons and A7 α and β protons that have 0.4−1 ppm upfield shifts from their random coil values that are attributed to the proximity of Y20 (Figure 7B and Supporting Information, Table 3). Similarly, consistent with the structure of PYY reported here, the γ and δ protons of P5 and the α and β protons of K4 are shifted by the presence of H26 and Y27, and the L30 and V31 γ and δ protons are moved upfield from their random coil values because of the proximity of Y1.

Our calculated structures reveal a PP-like fold for PYY. As shown in the structure overlay (Figure 7) and RMSD plot (Figure 8), a unique juxtaposition of the N-terminal and the C-terminal residues is defined by the distance restraints. The side chains of residues P5, A7, Y20, V24, H26, Y27, L30, and V31 are involved in the hydrophobic interaction between the N- and C-terminal portions of PYY (Figure 7B), and all of these residues have side-chain RMSDs of 1 Å or less (Figure 8, bottom). The backbone and side-chain portions of residues 1, 2, 8 to 14, 35, and 36 are less precisely defined by the NOE constraints as evidenced by their greater than 1

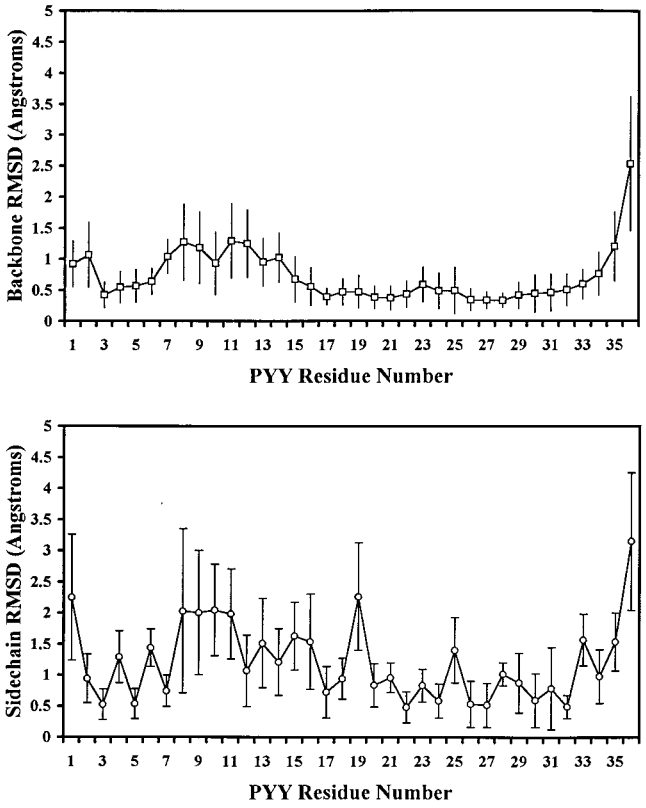

FIGURE 8: Plots of the root-mean-square deviation (RMSD) per residue for the backbone (top) and heavy atom (bottom) overlay of the 10 X-PLOR-calculated structures shown in Figure 7. The error bars denote the range of deviations from the mean structure for each residue of the 20 structure ensemble.

Å RMSDs (Figure 8). In addition, the side chains of residues K4, E6, R19, R25, and R33 all show a large range of conformations relative to the mean structure that is consistent with these residues being solvent exposed.

The monomeric PYY structure derived from the NOE data presented above is similar to the previously determined structure of aPP (*34*; Brookhaven Protein Data Bank, 1PPT). The 3D conformation of aPP can be described as a polyproline type II helix for residues 1−9, a β-turn from positions 10 to 14, and an amphipathic α-helix from residues 15 to 31. For aPP, the folded conformation is held together by hydrophobic interactions between the helical N- and C-terminal regions of the peptide. Similarly, in PYY the N- and C-termini are brought close together by hydrophobic interactions. In addition, in the PYY and aPP structures, residues R25−R33 are in a helical conformation with the same residues on the solution-exposed side of the helix (e.g., R25, N29, and R33). Furthermore, a similar alignment of the N-terminal residues with the C-terminal helix is also observed (e.g., residues 1 and 2 are close to residues 30 and 31, residues 3 and 5 are close to residue 27, and residue 20 is close to residues 7 and 8).

The structures calculated from the NOE data (Figure 7) have helical character for residues L17 to L23 and H26 to R33 with a break around residues V24 and R25. In the aPP crystal structure the helical segment extends uninterrupted from E15 to V31 (these differences are attributed to the sequence differences in the two peptides). It is not surprising that the tertiary structures of PYY and PP can vary in the turn region because others have shown that NPY analogues missing this portion of the molecule remain potent agonists (*35*, *36*).

For the turn region of the PYY structure overlay, the chemical shift difference data (Figure 3) and the NOE connectivity data (Figure 5) for residues E15 to L24 suggest helical character. Furthermore, the lowest energy structures with no distance violations were calculated after the upper boundaries of the distance restraints were increased and a set distance restraints that were regularly violated were removed. These data are consistent with the occurrence of chemical exchange between multiple conformations (e.g., helix and random coil) in this region of the peptide. In this model, the concentration of the helical form is sufficient for the chemical shifts and some of the NOE data to reflect the presence of a helix. Concomitantly, the alternate structures contribute to the observed NOEs in such a way to preclude a unique definition of the structure of these turn residues in the calculations where NOEs from both forms or an average of NOE values are present. For example, the observed NOE from interresidue NH to $C_\alpha H$ magnetization transfer in a helical conformation is weak while in a extended chain conformation the NH to $C_\alpha H$ NOE is strong; the concentrated weighted average of these two conformations may yield a NOE value that is too strong for a helical conformation.

To identify the major conformer in the flexible turn region of PYY, the upper bounds of the distance restraints were made larger and those constraints that consistently violated the new larger boundaries were removed. Because the remaining distance restraints found in the turn region represent the majority of the observed NOEs and had no distance violations, we propose that the final structure overlay (Figure 7) represents the conformer that is present in the highest concentration. By contrast, the structures of residues 3−8 and 25−33 were similar, had no NOE-based distance violations, had low energies, and had small RMSDs in all of the calculations, indicating an unique stable structure for the N- and C-terminal juxtaposition of PYY.

CONCLUSIONS

Despite their limited (ca. 50%) primary sequence homology, it has been assumed by numerous investigators that PYY and NPY have the same structure as aPP (*36*−*38*). Unfortunately, no high-resolution solution structure of monomeric PYY or NPY has been available. For NPY, this is because the peptide has a propensity to form multimers at concentrations necessary to perform structural studies. For PYY, no tertiary structure studies in aqueous solution had been performed.

In previous work, we found that PYY is mainly monomeric in solution at millimolar concentrations (*17*). The monomer−dimer dissociation constants compiled in Table 1 establish that at physiological concentrations (nanomolar) PYY and NPY will be almost entirely monomers. Thus, in this work we were able to solve the solution-state tertiary structure of PYY in a form that is probably the conformation that binds to Y receptors. We establish that the assumption of a PP-fold-like structure for PYY is valid. Furthermore, the PYY structure presented here may be useful in the design of agonists and antagonists for the Y_1, Y_2, Y_5, and the PYY-preferring receptor subtypes.

SUPPORTING INFORMATION AVAILABLE

One table of chemical shift assignments and one table of long-range NOE interactions for PYY. This material is available free of charge via the Internet at http://pubs.acs.org.

REFERENCES

1. Grundemar, L. (1997) in *Neuropeptide Y and drug development* (Grundemar, L., and Bloom, S. R., Eds.) pp 1−14, Academic Press, San Diego.
2. Fuhlendorff, J., Johansen, N. L., Melberg, S. G., Thogersen, H., and Schwartz, T. W. (1990) *J. Biol. Chem. 265*, 11706−11712.
3. Li, X., Sutcliffe, M. J., Schwartz, T. W., and Dobson, C. M. (1992) *Biochemistry 31*, 1245−1253.
4. Blomqvist, A. G., and Herzog, H. (1997) *Trends Neurosci. 20*, 294−298.
5. Wahlestedt, C., Regunathan, S., and Reis, D. J. (1991) *Life Sci. 50*, PL-7−PL-12.
6. Gehlert, D. R. (1994) *Life Sci. 55*, 551−556.
7. Wan, C. P., and Lau, B. H. S. (1995) *Life Sci. 56*, 1055−1064.
8. Bard, J. A., Walker, M. W., Branchek, T. A., and Weinshank, R. L. (1995) *J. Biol. Chem. 270*, 26762−26765.
9. Nakamura, M., Sakanaka, C., Aoki, Y., Ogasawara, H., Tsuji, T., Kodama, H., Matsumoto, T., Shimizu, T., and Noma, M. (1995) *J. Biol. Chem. 270*, 30102−30110.
10. Gehlert, D. R., Beavers, L. S., Johnson, D., Gackenheimer, S. L., Schober, D. A., and Gadski, R. A. (1996) *Mol. Pharmacol. 49*, 224−228.
11. Gehlert, D. R., Schober, D. A., Beavers, L., Gadski, R., Hoffman, J. A., Smiley, D. L., Chance, R. E., Lundell, I., and Larhammar, D. (1996) *Mol. Pharmacol. 30*, 112−118.
12. Gerald, C. M., Walker, M. W., Criscione, L., Gustafson, E. L., Batzl-Hartmann, C., Smith, K. E., Vaysse, P., Durkin, M. M., Laz, T. M., Linemeyer, D. L., Schaffhauser, A. O., Whitebread, S., Hofbauer, K. G., Taber, R. I., Branchek, T. A., and Weinshank, R. L. (1996) *Nature 382*, 168−171.
13. Hu, Y. B., Bloomquist, B. T., Cornfield, L. J., DeCarr, L. B., Flores-Riveros, J. R., Friedman, L., Jiang, P., Lewis-Higgins, L., Sadlowski, Y., Schaefer, J., Velazques, N., and McCaleb, M. L. (1996) *J. Biol. Chem. 271*, 26315−26319.
14. Kalivas, P. W., Duffy, P., and Latimer, L. G. (1987) *J. Pharmacol. Exp. Ther. 242*, 757−763.
15. Mannon, P. J., Hernandez, E. J., Mervin, S. J., Vigna, S. R., and Taylor, I. L. (1993) *Peptides 14*, 567−572.
16. Weiland, H. A., Willim, K., and Doods, H. N. (1995) *Peptides 16*, 1389−1394.
17. Keire, D. A., Mannon, P., Kobayashi, M., Walsh, J. H., Solomon, T. E., and Reeve, J. R., Jr. (2000) *Am. J. Physiol.* (in press).
18. Grandt, D., Teyssen, S., Schimiczek, M., Reeve, J. R., Jr., Feth, F., Rascher, W., Hirche, H., Singer, M. V., Layer, P., Goebell, H., Ho, F. J., and Eysselein, V. E. (1992) *Biochem. Biophys. Res. Commun. 186*, 1299−1306.
19. Grandt, D., Schimiczek, M., Rascher, W., Feth, F., Shively, J., Lee, T. D., Davis, M. T., Reeve, J. R., Jr., and Michel, M. C. (1996) *Regul. Pept. 67*, 33−37.
20. Beck-Sickinger, A. G., Wieland, H. A., Wittneben, H., Willim, K., Rudolf, K., and Jung, G. (1994) *Eur. J. Biochem. 225*, 947−958.
21. Darbon, H., Bernassau, J., Deleuz, C., Chenu, J., Roussel, A., and Cambillau, C. (1992) *Eur. J. Biochem. 209*, 765−771.
22. Monks, S. A., Karagianis, G., Howlett, G. J., and Norton, R. S. (1996) *J. Biomol. NMR 8*, 379−390.
23. Wuthrich, K. (1986) *NMR of Proteins and Nucleic Acids*, John Wiley and Sons, New York.
24. Braunschweiler, L., and Ernst, R. R. (1983) *J. Magn. Reson. 53*, 521−528.
25. Jeener, J., Meier, B. H., Bachmann, P., and Ernst, R. R. (1979) *J. Magn. Reson. 71*, 4546.
26. Rance, M., Sorensen, O. W., Bodenhausen, G., Wagner, G., Ernst, R. R., and Wuthrich, K. (1983) *Biochem. Biophys. Res. Commun. 117*, 479−485.
27. States, D. J., Haberkorn, R. A., and Ruben, D. J. (1982) *J. Magn. Reson. 48*, 286.
28. Brunger, A. T. (1992) *X-PLOR: Version 3.1, A System for X-ray Crystallography and NMR*, Yale Unviersity Press, New Haven, CT.
29. Wuthrich, K., Billeter, M., and Braun, W. (1983) *J. Mol. Biol. 169*, 949−961.
30. Nigles, M., Clore, G. M., and Gronenborn, A. M. (1988) *FEBS Lett. 2*, 317−324.
31. Saudek, V., and Pelton, J. T. (1990) *Biochemistry 29*, 4509−4515.
32. Wishart, D. S., Sykes, B. D., and Richards, F. M. (1992) *Biochemistry 31*, 1647−1651.
33. Perkins, S. J., and Wuthrich, K. (1979) *Biochim. Biophys. Acta 576*, 409−423.
34. Blundell, T. L., Pitts, J. E., Tickle, S. P., and Wu, C. W. (1981) *Proc. Natl. Acad. Sci. U.S.A. 78*, 4175−4179.
35. Beck, A., Jung, G., Gaida, W., Koppen, H., Lang, R., and Schnorrenberg, G. (1989) *FEBS Lett. 244*, 119−122.
36. Krstenansky, J. L., Owen, T. J., Buck, S. H., and Hagaman, K. A. (1989) *Proc. Natl. Acad. Sci. U.S.A. 86*, 4377−4381.
37. Glover, I. D., Barlow, D. J., Pitts, J. E., Wood, S. P., Tickle, I. J., Blundell, T. L., Tatemoto, K., Kimmel, J. R., Wollmer, A., Strassburger, W., and Zhang, Y. (1984) *Eur. J. Biochem. 142*, 379−385.
38. Allen, J., Novotny, J., Martin, J., and Heinrich, G. (1987) *Proc. Natl. Acad. Sci. U.S.A. 84*, 2532−2536.
39. Minakata, H., Taylor, J. W., Walker, M. W., Miller, R. J., and Kaiser, E. T. (1989) *J. Biol. Chem. 264*, 7907−7913.
40. Cowley, D. J., Hoflack, J. M., Pelton, J. T., and Saudek, V. (1992) *Eur. J. Biochem. 205*, 1099−1106.
41. Doughty, M. B., and Hu, L. (1993) *Biopolymers 33*, 1195−1206.
42. Nordmann, A., Blommers, M. J. J., Fretz, H., Arvinte, T., and Drake, A. F. (1999) *Eur. J. Biochem. 261*, 216−226.

BI992576A